

# Estimation of along-track velocity of road vehicles in SAR data

G. Palubinskas<sup>a</sup>, F. Meyer<sup>a</sup>, H. Runge<sup>a</sup>, P. Reinartz<sup>a</sup>, R. Scheiber<sup>b</sup>, R. Bamler<sup>a</sup>

DLR German Aerospace Center

<sup>a</sup>Remote Sensing Technology Institute

<sup>b</sup>Microwaves and Radar Institute

Oberpfaffenhofen, 82234 Wessling, Germany

[Gintautas.Palubinskas@dlr.de](mailto:Gintautas.Palubinskas@dlr.de)

## ABSTRACT

At the German Aerospace Center, DLR, an automatic and operational traffic processor for the TerraSAR-X ground segment is currently under development. The processor comprises the detection of moving objects on ground, their correct assignment to the road network, and the estimation of their velocities. Since traffic flow parameters are required for describing dynamics and efficiency of transportation, the estimation of the velocity of detected ground moving vehicles is an important task in traffic research science. In this paper we show for TerraSAR-X simulated data how the along-track velocity component of a moving vehicle can be derived indirectly by processing SAR data with varying frequency modulation (FM) rates and exploiting the specific behavior of the vehicle's signal through the FM rate space. An airborne ATI-SAR campaign with DLR's ESAR sensor has been conducted in April 2004 in order to investigate the different effects of ground moving objects on SAR data and to acquire a data basis for algorithm development and validation. Several test cars equipped with GPS sensors as well as vehicles of opportunity on motorways with unknown velocities were imaged with the radar under different conditions. To acquire reference data of superior quality, all vehicles were simultaneously imaged by an optical sensor on the same aircraft allowing their velocity estimation from sequences of images.

The paper concentrates on the estimation of along-track velocities of moving vehicles from SAR data. Velocity measurements of vehicles in controlled experiments are presented, including data processing, comparison with GPS and optical reference data and error analysis.

**Keywords:** Ground moving target detection, SAR azimuth focusing, matched filter bank, velocity estimation

## 1. INTRODUCTION

The German radar satellite TerraSAR-X is a high resolution, dual receive antenna (DRA) SAR satellite, which will be launched in spring 2006 as described by Buckreuss<sup>1</sup> and Mittermayer<sup>2</sup>. Since it will have the capability to measure the velocity of moving targets (DRA mode), the acquired interferometric data can be useful for traffic monitoring applications on a global scale.

DLR has started already the development of a processing system, called "traffic processor", which will detect cars, measure their speed and assign them to their corresponding road from which they are displaced due to the train-off-the-track effect. For more details see publications of Runge<sup>3,4</sup>, Meyer<sup>5</sup> and Suchandt<sup>6,7</sup>. The estimation of the velocity of detected moving vehicles is an important task in traffic research science. Different approaches have already been developed to estimate the across-track velocity component from SAR data, e.g. in Moreira<sup>8</sup>, Breit<sup>9</sup> and Gierull<sup>10</sup>. Some of them exploit the effect that vehicles moving in across-track direction do not appear at their correct image position but are displaced in along-track direction (train-off-the-track effect). Other methods are based on along-track interferometry (ATI), provided that a SAR system with at least two channels is available. The estimation of the second velocity component, the along-track velocity, is less investigated. In this paper it will be shown how the along-track velocity component of a moving vehicle can be derived indirectly by processing SAR data with varying frequency modulation (FM) rates and exploiting the specific behavior of the vehicle's signal through the FM rate space (see, e.g., Gierull<sup>10</sup>).

In SAR processing it is well known that vehicles moving in along-track appear smeared in azimuth direction, when nominal SAR azimuth focusing (stationary world assumption) is performed. Along-track motion changes the relative velocity of sensor and vehicle resulting in a change of the FM rate and consequently in a mismatch of the vehicle's signal and the stationary world matched filter. The extent of this defocusing is directly proportional to the along track velocity of the target. Re-sharpening of defocused moving targets in SAR images is achieved by varying the FM rate of the

matched filter. Besides the maximizing of the signal's peak energy, this yields additionally an indirect measure of the along-track velocity component of the vehicle. Maximization of the peak energy is a necessary step to optimize the detection of moving vehicles and to reduce biases in the across-track velocity determined from the ATI phase.

First, a short introduction to the theory of FM rate processing will be given, then, the DLR experimental radar sensor ESAR, used for the acquisition of SAR data is introduced, and the experiment setups are explained in details. In the following section results of along-track velocity estimation for four controlled cars on the runway are presented, including data processing, comparison with GPS reference data and error analysis.

## 2. THEORY

The phase signal of a point scatterer imaged by a passing SAR satellite is given by

$$u(t) = \exp\left\{-j\frac{4\pi}{\lambda}R(t)\right\}$$

where  $\lambda$  is the wavelength of the sensor and  $R(t)$  the range history of the target during illumination time. For easier computation this equation is usually approximated by

$$u(t) = \exp\{j\pi FMt^2\}$$

with

$$FM = -\frac{2}{\lambda} \frac{d^2}{dt^2} R(t) = -\frac{2(v_s - v_x)^2}{\lambda R_0} = FM(v_x)$$

being the frequency modulation rate of a linear moving point scatterer with a velocity in azimuth direction  $v_x$  (defined positive in flight direction). In this equation,  $R_0$  is the range of closest approach and  $v_s$  the sensor's forward velocity and, thus,  $(v_s - v_x)$  is the relative velocity of sensor and point scatterer. This quadratic phase term corresponds to a spread of the backscattered energy of a point scatterer over many azimuth resolution cells. In order to obtain a focussed image this quadratic phase term has to be removed from the data. The compression is usually done based on the concept of matched filtering. The spectrum of an ideal matched filter is given by

$$H(f, v_x) = \exp\left(-j\pi \frac{1}{FM(v_x)} f^2\right),$$

where  $f$  is the frequency. In conventional SAR processing the scattering centers on the surface are usually assumed to be non-moving (i.e.  $|v_x| = 0$ ). This concept is commonly referred to as *stationary-world matched filtering*. If a moving object with a significant velocity component in azimuth direction (i.e.  $|v_x| > 0$ ) is imaged by the sensor, nominal SAR azimuth focusing with  $H(f, 0)$  causes a smearing in azimuth direction since the assumed relative velocity of sensor and target is wrong, resulting in a mismatch of the target's signal and the stationary-world matched filter. The degree of defocusing is proportional to  $|v_x|$ . By processing the SAR data with varying FM rates of the matched filter, a moving object, that appears defocused due to  $v_x$ , can be sharpened and its peak energy can be increased. Maximization of the peak energy is necessary to optimize the detection of moving targets and to reduce biases in the across-track velocity determined from the ATI phase. A corrective moving target post processing was performed with a matched filter  $H(f, v_x)/H(f, 0)$ , with  $v_x$  running over all possible along-track velocities for an analyzed scene.

## 3. DATA

DLR's airborne experimental SAR sensor ESAR was used in the flight campaigns for the acquisition of the radar image data. This system has been in use for different applications and has been continuously improved and extended over a period of more than 16 years by now. It is operated on a Do-228 aircraft. Detailed description of the sensor can be found in Scheiber<sup>11</sup>. Table 1 lists the main ESAR system parameters for the SAR experiments.

To locate vehicles in the radar images and to verify measurements optical reference data were recorded simultaneously with the SAR acquisition. The sensor platform additionally carried an optical Zeiss RMK-A camera, which took images at a sampling rate of about 0.3 Hz. These were processed to a resolution of 0.5 m and car positions and velocities were interactively extracted from sequences of images. The accuracy of these data was 2 m for the x,y-coordinates and about 5 km/h for the velocities. Details on the processing of the optical data can be found in Reinartz<sup>12</sup>.

Table 1: ESAR system parameters.

Parameter	Value
frequency band	X (9.6 GHz)
polarization	VV
wavelength	0.311 m
range bandwidth	100 MHz
pulse repetition frequency	1000 Hz
azimuth processing bandwidth	960 Hz
sensor forward velocity	88 m/s
altitude above ground	3940 m
incidence angle	20 – 60 deg
resolution (rg x az)	2 m x 0.08 m
SLC pixel spacing (rg x az)	1.50 m x 0.089 m

#### 4. EXPERIMENTS

The experimental data have been collected during the flight campaign on April 20<sup>th</sup>, 2004 over Oberpfaffenhofen, Germany. During this flight campaign interferometric (ATI) SAR data were collected for the polarization X-VV. The ground coverage of the data takes are shown in Fig. 1.

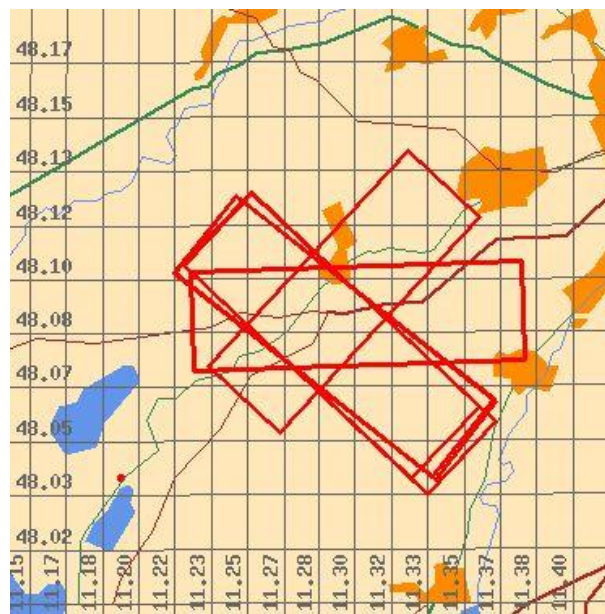


Figure 1: Footprints of SAR data takes for Oberpfaffenhofen campaign.

Four moving vehicles – all equipped with GPS receivers – covered a speed range from 5 to 37 km/h. These slow velocities had to be used in order to approximate the imaging situation of TerraSAR-X as close as possible. The involved cars were: Mercedes M (no.1), BMW 5 (no. 2), Mercedes Sprinter (no. 3) and VW T4 (no. 4) (see Fig. 2). Two of them (no. 2 and no. 3) were carrying corner reflectors, e.g. Lüneburg lens, on the top.

In this section it will be shown how a moving object, that appears defocused due to an along-track velocity, can be sharpened, its peak energy can be increased and even its along track velocity can indirectly be derived. Data from two flight strips with different headings are analyzed in the following sections.



Figure 2: Test cars used in the experiments.

#### 4.1 Along-track direction experiment

In this experiment the flight heading was almost parallel to the runway and only defocusing effects were expected in the SAR image. Figure 3 shows four test cars moving on the runway with different velocities in a nominally processed radar image (left) and a reference optical image (right). The radar signatures of the cars appear heavily defocused. Fortunately the cars can be sharpened, its peak energy can be increased and even their along track velocity can indirectly be derived.

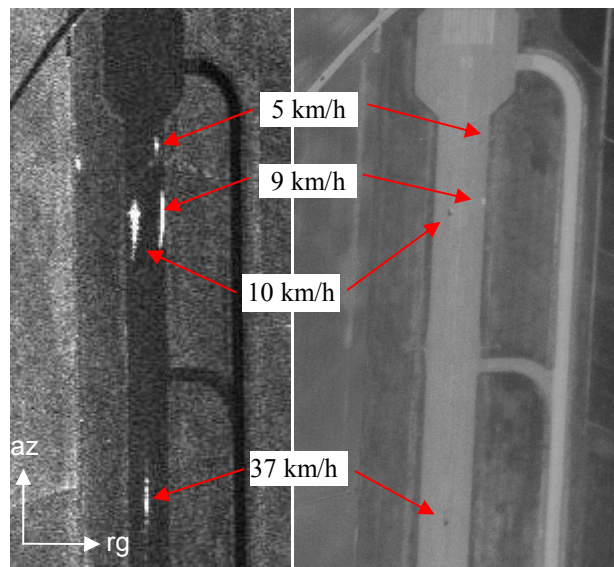


Figure 3: Test cars with different velocities on the runway in a nominally processed radar image (left) and a reference optical image (right).

This is done by processing the SAR data with varying FM rates of the matched filter, thereby exploiting the specific behavior of the target's signal through the FM rate space. Maximization of the peak energy is a necessary step to optimize the detection of moving targets and to reduce biases in the across-track velocity determined from the ATI phase. In our E-SAR experiment the data were processed with a "stationary world matched filter"  $H(f;0)$ , first. After this standard processing, a corrective moving target post processing is performed with a matched filter  $H(f;v_x)/H(f;0)$ , where  $v_x$  runs over all possible along-track velocities for the scene under investigation.

The effect of the FM rate technique is demonstrated in Figure 4. It shows five radar images processed with different FM rates for car no. 3 that travels with a velocity of 37 km/h. The moving car is focused correctly when a matched filter with a FM rate corresponding to 37 km/h is used. Hence, the along-track velocity component has been indirectly estimated!

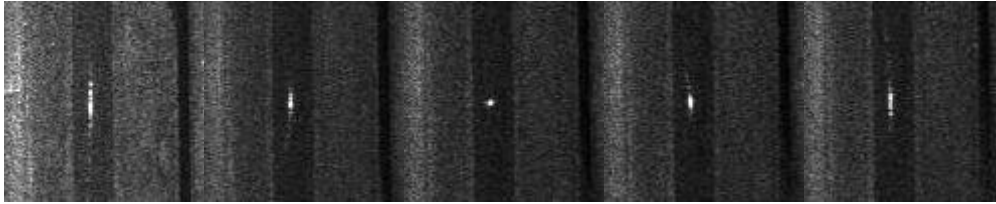


Figure 4: Five radar images of a car driving with a velocity of 37 km/h processed with FM rates adapted for 0, 20, 37, 50 and 70 km/h.

Finding the maximum in such a stack of images can be better illustrated in a plot as, e.g., presented in Figure 5. Here, again a car moving with 37 km/h speed is illustrated. A part of an azimuth line (vertical line) containing a car is extracted in all images processed with different FM rates and then all lines are stacked together to form an image. In the ideal case, the estimation of the velocity reduces to finding the maximum in such an image.

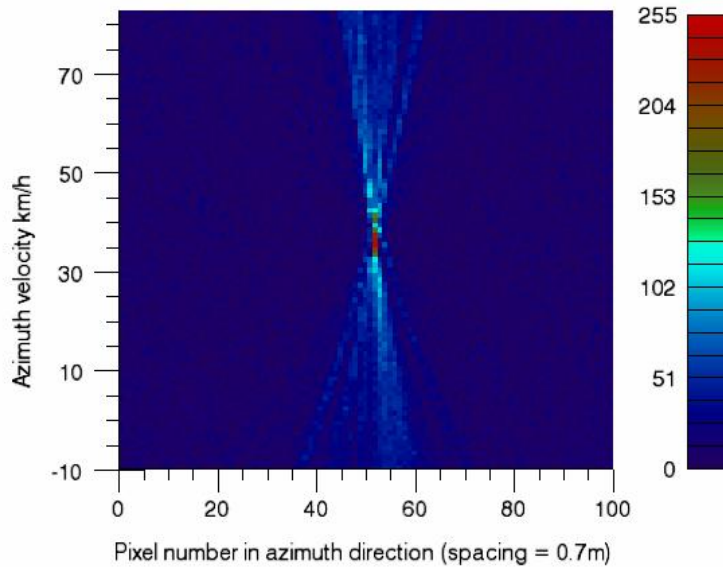


Figure 5: Azimuth lines containing a car moving with a speed of 37 km/h processed with different velocities.

In this paper we have used the simplest and fastest way to estimate the velocity. It required manual interaction to identify or to detect a car. Then, the maximum amplitude value of the analyzed small area around the car in each of the FM processed images was found. However, this solution is a sub-optimal one and the improvements are under investigation in Meyer<sup>13</sup>. Plots of such maximum values for each test car are shown in Fig 6. The peak of this curve corresponds to the estimated along-track velocity component. For example, for a car moving with  $v = 37$  km/h the estimated along-track velocity component is  $v_{FM} = 35.7$  km/h. So the car velocity on the runway can be calculated using the following formulae  $v = v_{FM} / \cos(\alpha)$ , where  $\alpha$  is the angle difference between the flight heading and the runway direction, which for this experiment was  $\alpha = 1.9^\circ$ . The analysis of the plots in Fig. 6 shows that finding the peak is not always a trivial task and requires further investigations.

The estimated velocities of the four test cars using the FM rate processing technique and comparison with GPS measurements are presented in Table 2. The difference of the FM estimate of the velocity to the GPS velocity (error) is below 5%, except for the car no. 1, where the wrong peak is found. For the latter case the error is about 30%.



Table 2: Estimated velocities for along-track direction experiment.

Car	Velocity FM (km/h)	Velocity GPS (km/h)	Difference	Difference %
1. Mercedes M	3.5	5.08	1.58	31.1
2. BMW 5	9.3	9.25	-0.05	-0.5
3. Mercedes Sprinter	9.9	10.23	0.33	3.2
4. VW T4	35.7	37.22	1.52	4.1

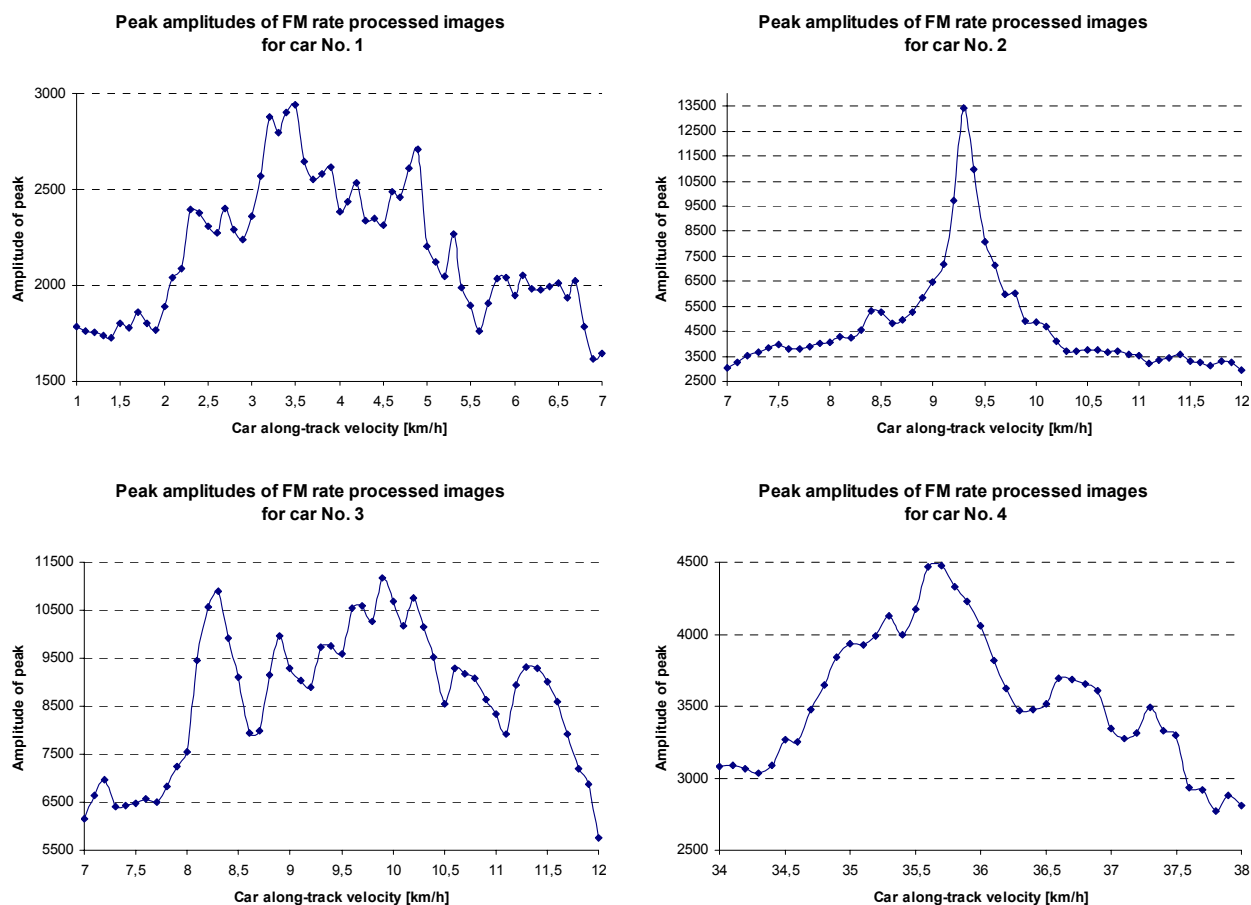


Figure 6: Peak amplitudes of FM rate processed images for four cars in the first experiment.

## 4.2 45° direction experiment

In this experiment the flight heading was about 45° to the runway, so both azimuth displacement and defocusing effects were expected in the SAR image. In this case the angle difference between the flight heading and the runway direction  $\alpha = 44^\circ$ .

Figure 7 shows four test cars driving on the runway with different velocities in a nominally processed radar image (left) and a reference optical image (right). The radar signatures of the cars appear heavily defocused and additionally displaced in azimuth direction. The car No. 4 could not be identified in the radar image because of the weak radar signature at this aspect angle (Palubinskas<sup>14</sup>) and high clutter values at that position, to which it was displaced.

The estimated velocities of the three test cars using the FM rate processing technique and comparison with GPS measurements are presented in Table 3. The estimation error is around 10%, except for the car no. 3, where the wrong peak is found. For the latter case the error is about 30%.

Again the peak amplitude plots found in FM processed images are presented in Fig. 8.

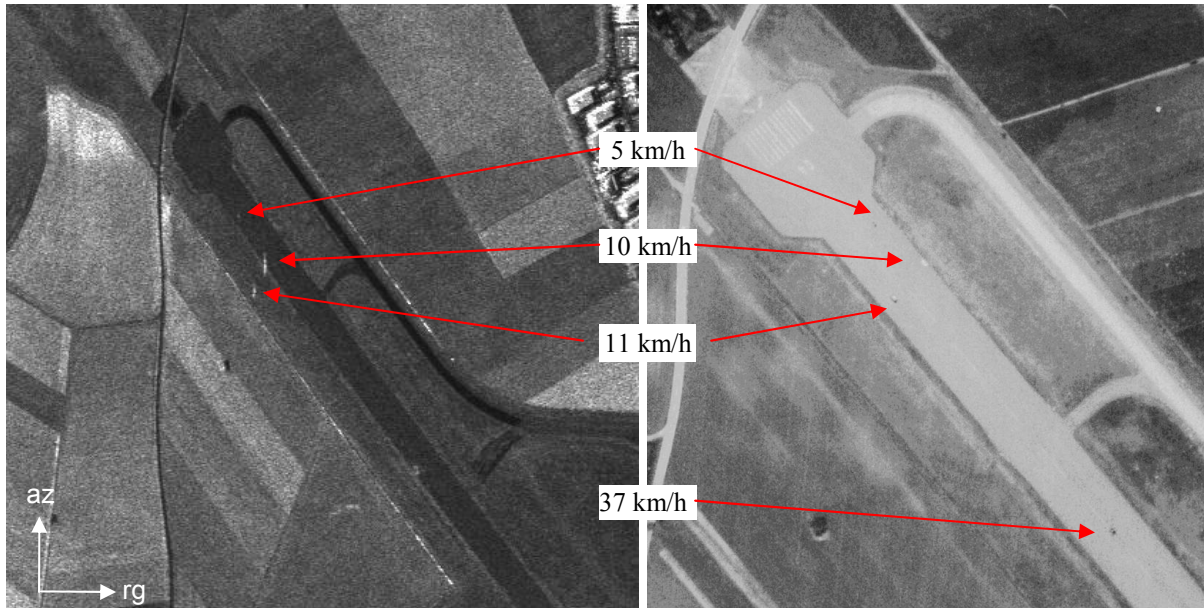


Figure 7: Test cars with different velocities on the runway in a nominally processed radar image (left) and a reference optical image (right).

Table 3: Estimated velocities for 45° experiment.

Car	Velocity FM (km/h)	Velocity GPS (km/h)	Difference	Difference %
1. Mercedes-M	4.43	4.96	0.53	10.7
2. BMW	8.58	9.52	0.94	9.9
3. Mercedes-Sprinter	7.06	10.65	3.59	33.7
4. VW-T4	-	37.05	-	-

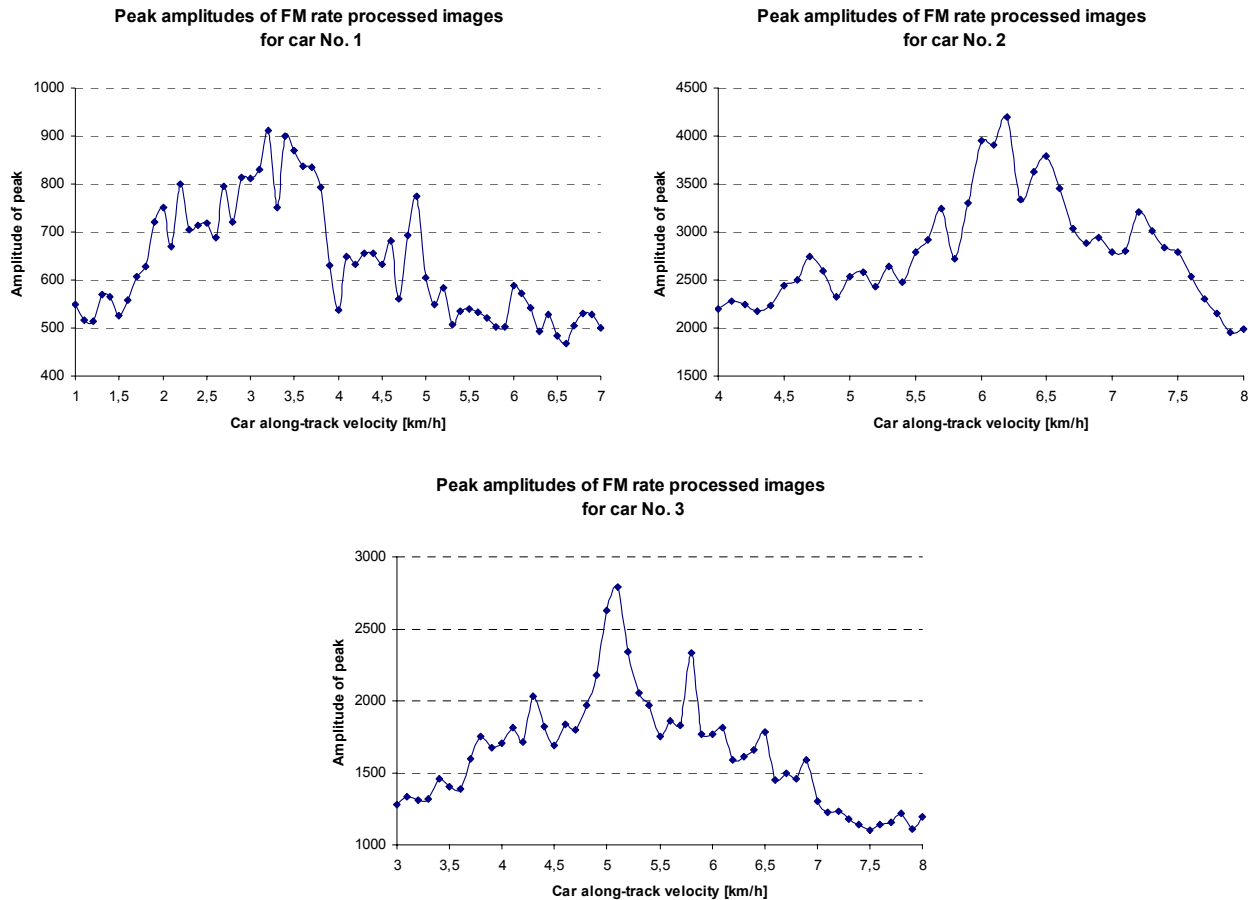


Figure 8: Peak amplitudes of FM rate processed images for four cars in the second experiment.

## 5. DISCUSSION

Experiments with test cars show the potential of the proposed method to estimate the along-track velocity in SAR images. The estimation accuracy varies from 95% for purely along-track direction experiment to 90% for 45° direction experiment, except few errors up to 30%, maybe due sub-optimal solution.

The FM rate processing requires additional computation power, which can be reduced significantly by using carefully selected regions of interest (ROI).

Availability of a priori information, such as a road GIS, can allow additionally the estimation of the across-track velocity from the amount of azimuth displacement. So the velocity of a vehicle can be estimated from only one SAR image.

Automatic detection techniques of moving vehicles are under investigation and will substitute the manual interaction.

## 6. CONCLUSION

In the described airborne SAR ATI experiments the along-track effect of moving objects was investigated and different vehicles in controlled situations were imaged with the ESAR sensor. The experimental cars could easily be detected in the SAR images and their speed was estimated quite accurately. The expected effect of defocusing was clearly observed and quantified. The analysis of cars on public roads is still going on, so the results could not be included in this paper.



## ACKNOWLEDGEMENTS

We would like to thank our colleague Helko Breit for theoretical discussions, Ralf Horn from DLR's Microwave and Radar Institute, for his efforts in planning the flight campaigns and data acquisition.

## REFERENCES

1. S. Buckreuss, W. Balzer, P. Mühlbauer, R. Werninghaus, and W. Pitz, "The TerraSAR-X Satellite Project," *Proc. of IEEE IGARSS'03 Conference*, pp. 3096–3098, 2003.
2. J. Mittermayer, and H. Runge, "Conceptual Studies for Exploiting the TerraSAR-X Dual Receive Antenna," *Proc. of IEEE IGARSS'03 Conference*, pp. 2140–2142, 2003.
3. H. Runge, and M. Ruhé, "Verkehrsmonitoring mit dem deutschen Fernerkundungssatelliten TerraSAR-X", *DLR Nachrichten* **106**, pp. 10–15, December 2003.
4. H. Runge, M. Eineder, G. Palubinskas, S. Suchandt, and F. Meyer, "Traffic monitoring with TerraSAR-X", in *Proc. of International Radar Symposium (IRS2005), 6-8 September, 2005, Berlin, Germany*, 2005. (in print)
5. F. Meyer, and S. Hinz, "The Feasibility of Traffic Monitoring with TerraSAR-X – Analyses and Consequences," *Proc. of IEEE IGARSS'04 Conference*, pp. 3096–3098, 2004.
6. S. Suchandt, G. Palubinskas, H. Runge, M. Eineder, F. Meyer, and R. Scheiber, "An airborne SAR experiment for ground moving target identification", in *Proc. of ISPRS Hannover Workshop 2005 - High Resolution Earth Imaging for Geospatial Information, 17-20 May, 2005, Hannover, Germany*, ISPRS, vol. XXXVI, part I/W3, 2005.
7. S. Suchandt, G. Palubinskas, R. Scheiber, F. Meyer, H. Runge, P. Reinartz, and R. Horn, "Results from an Airborne SAR GMTI Experiment supporting TSX Traffic Processor Development", in *Proc. of IEEE International Geoscience and Remote Sensing Symposium (IGARSS'05), 25-29 July, 2005, Seoul, Korea*, IEEE, vol. IV, pp. 2949-2952, 2005.
8. J.R. Moreira, W. Keydel, "A New MTI SAR Approach Using the Reflectivity Displacement Method", *IEEE Trans. Geoscience and Remote Sensing*, vol. 33, No. 5, pp. 1238-1244, 1995.
9. H. Breit, M. Eineder, J. Holzner, H. Runge, and R. Bamler, "Traffic Monitoring using SRTM Along-Track Interferometry", in *Proc. of IEEE IGARSS 2003, 21-25 July, 2003, Toulouse, France*.
10. C.H. Gierull, and I. Sikaneta, "Ground Moving Target Parameter Estimation For Two-Channel SAR", in *Proc. of EUSAR 2004, 25-27 May, 2004, Ulm, Germany*, vol. 2, pp. 799-802.
11. R. Scheiber, A. Reigber, A. Ulbricht, K.P. Papathanassiou, R. Horn, S. Buckreuß, and A. Moreira, "Overview of Interferometric Data Acquisition and Processing Modes of the Experimental Airborne SAR System of DLR", *Proc. of IEEE IGARSS'99 Conference*, 1999.
12. P. Reinartz, T. Krauss, M. Pötzsch, H. Runge, and S. Zuev, "Traffic Monitoring with serial images from airborne cameras", in *Proc. of ISPRS Hannover Workshop 2005 - High Resolution Earth Imaging for Geospatial Information, 17-20 May, 2005, Hannover, Germany*, ISPRS, vol. XXXVI, part I/W3, 2005.
13. F. Meyer, S. Hinz, A. Laika, and R. Bamler, "Spaceborne traffic monitoring with dual channel synthetic aperture radar – theory and experiments", in *Proc. CVPR, San Diego, USA*, 2005.
14. G. Palubinskas, H. Runge, and P. Reinartz, "Radar signatures of road cars", in *Proc. of IEEE International Geoscience and Remote Sensing Symposium (IGARSS'04), 20-24 September, 2004, Anchorage, Alaska, USA*, IEEE, vol. II, pp. 1498-1501, 2004.